SDS Surfactants on Carbon Nanotubes: Aggregate Morphology

Naga Rajesh Tummala and Alberto Striolo*

The University of Oklahoma, School of Chemical, Biological and Materials Engineering, Norman, Oklahoma 73019

ABSTRACT Although carbon nanotubes have attracted enormous research interest, their practical application is still hindered, primarily, by the difficulty of separating them into samples monodispersed in diameter, chirality, and length. Recent advances show that ultracentrifugating carbon nanotube dispersions stabilized by surfactants is a promising route for achieving the desired separation. For further perfectioning this procedure it is necessary to know how surfactants adsorb on nanotubes of different diameters, which determines the nanotube—surfactant aggregate effective density and the nanotube—nanotube potential of mean force. Because only limited experimental data are available to elucidate these phenomena, we report here an extensive all-atom molecular dynamics study on the morphology of sodium dodecyl sulfate (SDS) surfactant aggregates adsorbed on (6,6), (12,12), and (20,20) single walled carbon nanotubes at room conditions. Our calculations reveal that the nanotube diameter is the primary factor that determines the morphology of the aggregates because of a competition between the entropic and energetic advantage encountered by the surfactants when they wrap one nanotube, and the enthalpic penalty faced during this process due to bending of the surfactant molecule. The data are in qualitative agreement with the neutron scattering results reported by Yurekli *et al*. [*J. Am. Chem. Soc*. 2004, *126*, 9902], and for the first time provide an atomic-level description helpful in designing better separation, as well as stabilization techniques for aqueous carbon nanotube dispersions.

KEYWORDS: molecular dynamics simulations · admicelles · density profiles

Single-walled carbon nanotubes (SWNTs) have attracted vast research attention in the last two decades because of seemingly unlimited intrinsic properties.[1−4] Several methods are now available for producing this material,[5−8] and the last barrier that prevents the widespread application of carbon nanotubes consists in the difficulty of separating them into samples monodispersed in diameter, chirality, and length. Significant advances have been accomplished in the recent years. O'Connell *et al*.[9] managed to suspend SWNTs in aqueous solutions and to remove carbon nanotube bundles using sodium dodecyl sulfate (SDS) surfactants by implementing ultracentrifugation procedures. The technique has been improved by Arnold *et al*.,[10] who, using bile salts such as sodium cholate in addition to SDS surfactants, demonstrated that it is possible to separate SWNTs on the basis of their diameter and electronic structure. Nair *et al*.[11] demonstrated that the number of surfactant molecules adsorbed on each SWNT causes the effective nanotube−surfactant complex density to change, and that this density change causes the separation of nanotubes during ultracentrifugation. Further, recent data by Niyogi *et al*.[12] show that adding electrolytes to SWNTs-SDS systems improves the fractionation of SWNTs using density-gradient ultracentrifugation methods. On the basis of these recent advances, it is clear that understanding how surfactants adsorb on SWNTs of various diameters will lead to further advancements in this field.

Unfortunately, however, it is still not clear how surfactants self-assemble on carbon nanotubes. It was postulated that the carbon nanotube−surfactant complexes resemble micelles in which the carbon nanotube forms the core and the surfactants extend radially from the core.[13−15] Another proposed morphology was one in which surfactant hemimicellar aggregates cover the carbon nanotubes.[16,17] The latter possibility has been challenged by energetic arguments discussed by Matarredona *et al*.,[18] and it seems unlikely to occur. To the best of our knowledge, the only experimental assessment on the morphology of surfactant aggregates adsorbed on carbon nanotubes is that reported by Yurekli *et al*.,[19] who used neutron scattering to characterize SWNTs dispersed in aqueous solutions with the aid of SDS surfactants at three concentrations. The experimental data do not support any ordered surfactant aggregate structure on the SWNTs, but rather suggest the formation of disordered aggregates. Because these results are at odds with the

*Address correspondence to astriolo@ou.edu.

Received for review November 16, 2008 and accepted February 11, 2009.

Published online February 19, 2009.
10.1021/nn8007756 CCC: $40.75

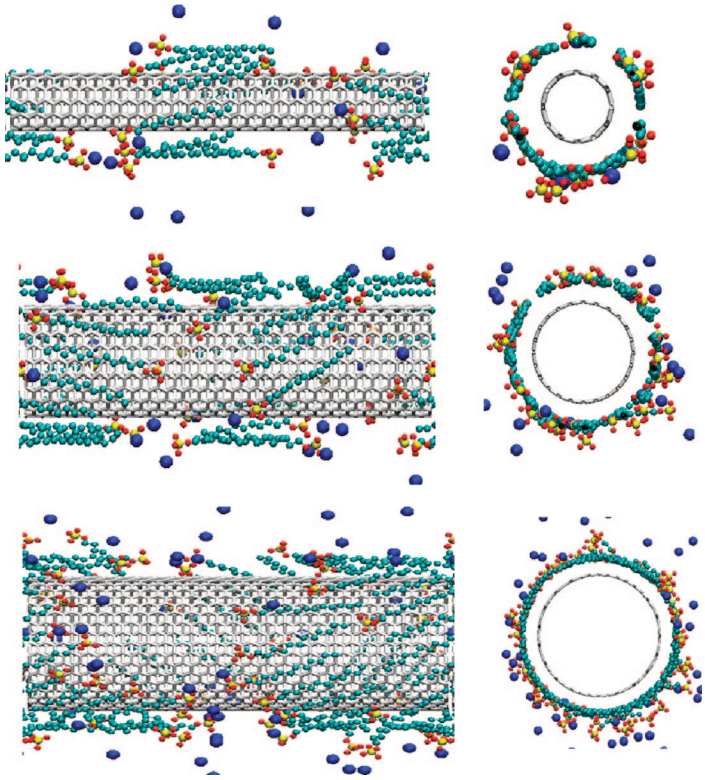

Figure 1. Side (left panels) and front views (right panels) of representative snapshots for (6,6) (top), (12,12) (center), and (20,20) SWNTs (bottom) covered by SDS surfactants at a surface density of 0.98 nm^2 per headgroup. Blue spheres are Na^+ ions. Cyan spheres are either CH_2 or CH_3 groups in the surfactant tails. Red and yellow spheres are oxygen and sulfur atoms in the SDS surfactant heads. Water molecules are not shown for clarity.

information available for the morphology of SDS aggregates on graphite,[20−23] they clearly indicate that the curvature of the solid support affects the morphology of adsorbed SDS aggregates. If this is the case, then the morphology of surfactant aggregates formed on SWNTs depends not only on surfactant concentration, temperature, and ionic strength, but also on nanotube diameter and chirality, possibly allowing for a precise separation of SWNTs dispersions into monodispersed samples. Further, it is likely that the molecular architecture of the surfactants (*i.e.*, linear alkyl chain *vs* branched chain containing benzene rings) determines how individual surfactants adsorb on SWNTs of given diameter, which is the principle employed, for example, to design cyclic peptides to selectively stabilize SWNTs in aqueous suspensions.[24]

A detailed understanding of the equilibrium structure of surfactant aggregates adsorbed on SWNTs of various diameters is necessary for improving separation techniques. Such understanding will not only improve the ultracentrifugation technique of Arnold *et al.*,[10] but is also necessary for correctly predicting the effective potential of mean force between carbon nanotubes in aqueous surfactant solutions. For the purposes of predicting the nanotube−nanotube potential of mean force, Patel and Egorov[25] proposed a disordered, yet uniform along the nanotube axis, distribution of surfactants around one carbon nanotube. However it is possible that local density fluctuations affect the pair potential of mean force, as suggested for example by our recent simulations on colloidal systems.[26−29] More importantly, understanding and visualizing the molecular arrangement of surfactants adsorbed on SWNTs of various diameters will allow us to understand the driving forces responsible for determining the aggregate morphology, thus leading to the design of surfactants more effective for stabilizing aqueous SWNTs dispersions.

Because of the technical limitations typically encountered by experimental methods at the nanoscale and because of the simplification necessary for applying density functional methods and coarse-grained simulations, molecular simulations conducted at the all-atom level offer the optimum compromise for securing progress in this field. One limitation typical for all-atom molecular dynamics simulations is that due to the currently available computational resources, it is only possible to simulate large systems for a few tens of nanoseconds. This requires the number of surfactant molecules near one SWNT to be treated as an input parameter in the simulations. The simulations are then conducted for a time sufficiently long to assess the equilibrium structure for the adsorbed aggregates.

We present here the first simulation results obtained for SDS surfactants adsorbed on (6,6), (12,12), and (20,20) SWNTs at room conditions, and we compare them to the structures proposed in the literature. Specifically, we analyze the effect of surface density and that of SWNT diameter on the aggregate morphology. The simulation results discussed herein are obtained from running all-atom molecular dynamics simulations for 50 ns. The results do not change over the last 30 ns of simulation time, and only those collected during the last 10 ns are presented in what follows. Simulation details are reported at the end of the text. The surfactant surface densities considered are consistent with the experimental data reported by Strano *et al.*,[30] Yurekli *et al.*,[19] and by Matarredona *et al.*,[18] although precise surfactant adsorption isotherms on SWNTs monodispersed in diameter are at present not available.

RESULTS AND DISCUSSION

Representative simulation snapshots for (6,6), (12,12), and (20,20) SWNTs covered by SDS surfactants are shown in Figures 1 and 2. In Figure 1 the surface area per surfactant headgroup is 0.98 nm^2 in the three nanotubes considered. The surface area per surfactant headgroup decreases in Figure 2, where it is 0.44, 0.49, and 0.81 nm^2 on (6,6), (12,12), and (20,20) SWNTs, respectively. Visual analysis suggests that the morphology of adsorbed aggregates depends on the surface coverage, as expected, but also, and more significantly,

on the SWNTs diameter. At low surface coverage (Figure 1) SDS surfactants on (6,6) SWNTs form "rings" in which the surfactants lie parallel or antiparallel to each other and parallel to the nanotube axis. As the SWNTs diameter increases the SDS surfactants still lie predominantly flat on the nanotube surface, but the surface coverage appears more uniform than that observed on the (6,6) SWNTs. The orientation of the adsorbed surfactants with respect to the nanotube axis also changes as the nanotube diameter increases, as discussed at length below.

The different structures of the SDS assemblies on the SWNTs at high surface area per headgroup (Figure 1) are due to a competition between various factors, including surfactant−nanotube and surfactant−surfactant interactions. One of the leading effects seems to be the rigidity of the SDS molecule. SDS surfactants on graphite at low surface coverage (*i.e.*, high surface area per headgroup) preferentially lie along one of the three α symmetry axes to maximize the number of contacts between the surfactant tail and the carbon atoms in graphite.[21] Because the SWNTs are obtained by rolling one graphene sheet into one cylinder, in the SWNTs considered here one of the α symmetry axes is parallel to the SWNTs axes. Thus if the SDS surfactants lie along one of the α axes, they can be either parallel to the SWNTs axis, or they must wrap the nanotubes. Because of entropic reasons, both possibilities should occur. However, when one SDS molecule wraps around a narrow tube, it has to bend, encountering an energetic barrier (SDS is rather straight). Our simulations show that the entropic advantage of wrapping the nanotubes forming various angles with the nanotube axis is not sufficient to balance the energetic penalty encountered to bend the SDS molecule around the narrow (6,6) SWNTs. As the nanotube diameter increases, it becomes easier and easier for the adsorbed SDS to wrap the SWNTs not only because smaller bending of the SDS molecule is necessary, but also because the number of surfactant tail−carbon atoms contacts increases when the SDS surfactants lie along the β symmetry axes, which form an angle with respect to the nanotube axes. This latter effect is nanotube specific, that is, it occurs on the (20,20) SWNTs, but not on the other nanotubes considered here.

The morphology of the surfactant aggregates at high surface area per headgroup (Figure 1) is important because such aggregates provide a template to those formed at higher densities (Figure 2). On the (6,6) SWNTs the SDS surfactants adsorb on top of the rings formed at low density, and they yield admicelles that, although seem ordered at contact with the nanotube, lack any long-range order. Evidently, as the SDS coverage increases, the adsorbed aggregate structure depends predominantly on SDS−SDS interactions. It is also worth pointing out that some small regions of the (6,6) SWNT surface remain exposed to water even at this large surfactant surface density. This is probably because the adsorbed SDS surfactants find it more favorable to maximize the SDS−SDS interactions than spread evenly on the SWNTs surface. In fact, because the SDS surfactants remain in large part parallel to the SWNTs, by spreading evenly on the SWNTs they would decrease the SWNT area in contact with water, but they would increase the tail area in contact with water, with no overall free-energy benefit. On the (12,12) SWNTs the SDS surfactants seem to form a continuous first layer of adsorbed surfactants at contact with the nanotube surface, and excess SDS molecules agglomerate forming a multilayered structure. Although no long-range order is visible, each surfactant within these admicelles appears parallel or antiparallel to its neighbors. On the (20,20) SWNTs the surface coverage was not large enough to provide complete coverage of the nanotube surface. Nevertheless, the surfactants would in some case prefer to agglomerate together rather than spread over the entire available surface.

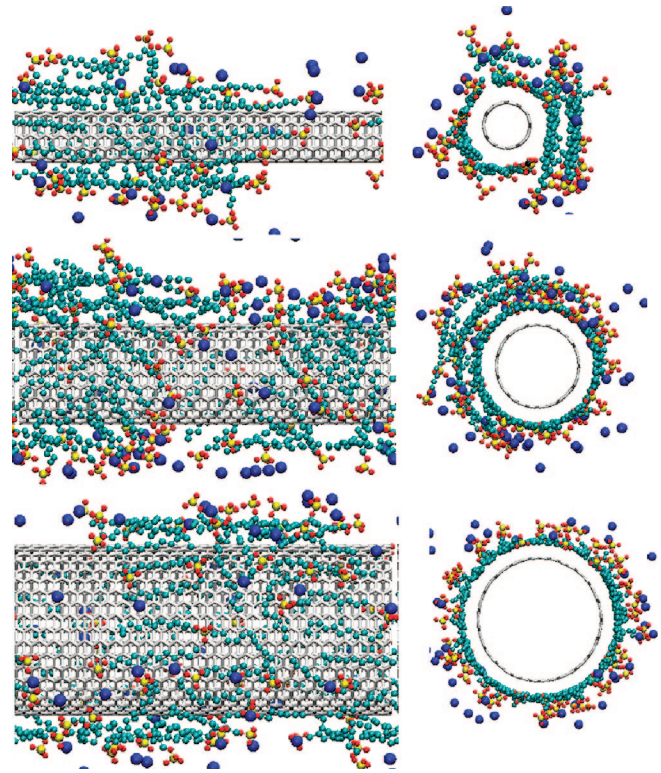

Figure 2. Same as Figure 1, but for SDS surfactants at a surface density of 0.44, 0.49, and 0.81 nm^2 per headgroup on (6,6), (12,12), and (20,20) SWNTs, respectively. Water molecules are not shown for clarity.

The effects just described are due to a combination of tail−tail and tail−nanotube hydrophobic interactions. However also counterion-condensation phenomena, which, as we described earlier,[20] contribute in shielding the electrostatic repulsion between surfactant heads and effectively bring them close to each other, and intrinsic properties of the straight SDS mol-

ecules seem to play a major role in determining the morphology of the adsorbed surfactant aggregates. It is worth pointing out that the structure of SDS aggregates formed on the SWNTs considered here are completely different compared to those obtained on flat graphite surfaces. As previously shown in the literature,[20,22,31] molecular dynamics simulations, in agreement with experimental AFM data,[23] for ionic surfactants on graphite yield hemicylindrical aggregates. Because the force fields implemented in this work are exactly the same as those used in our previous work for SDS on graphite, the morphology of the substrate (*i.e.*, cylindrical *vs* flat) is the only possible cause for the differences observed in surfactant aggregates morphology. Clearly, the SWNTs curvature makes it energetically unfavorable for the SDS surfactants to form hemicylindrical admicelles. The results just discussed suggest that by appropriately designing surfactants at the molecular level it should be possible to completely wrap SWNTs of specific diameter. A similar approach has been successfully demonstrated by Ortiz-Acevedo *et al.*,[24] who designed circular peptides that selectively associate to carbon nanotubes of given diameter. Our results may also explain why bile salts tend to yield more stable aqueous SWNTs dispersions, although additional simulations are necessary.

In all the cases considered in Figures 1 and 2 the SDS aggregates do not show long-range order, in qualitative agreement with the experimental data of Yurekli *et al.*,[19] and certainly cannot be described in terms of the ordered micellar structures postulated earlier in the literature.[13,14,16−18] In addition, we point out that the snapshots in Figures 1 and 2 do not agree with a completely disordered structure either, as it may be inferred from the interpretation of the neutron scattering data of Yurekli *et al*. In fact, our simulations suggest that SDS surfactants cover the SWNTs sometimes only partially, and that a short-ranged order is present within the individual micellar structures. Because of a competition of forces, as described above, the individual SDS surfactants tend to lie on the SWNT surface, especially at low surface density. Additionally, the SDS surfactants adsorbed on the (6,6) SWNTs seem constantly parallel to the nanotube axis, whereas those adsorbed on the (20,20) SWNTs lie on the surface forming a slanted angle with the nanotube axis. This different orientation is more visible at low surface density (Figure 1), but it is nevertheless present at all conditions considered herein. In Figure 3, top panel, we quantify the orientation of SDS surfactants adsorbed on the SWNTs at low surface density by reporting the probability density of observing various angles between the SDS surfactants and the SWNTs axis. When the angle is either 0° or 180°, the surfactants are parallel to the SWNTs axis, when the angle is 90° the surfactants lie perpendicularly to the nanotube axis. The results clearly show that while SDS surfactants lie parallel or antiparallel to the (6,6)

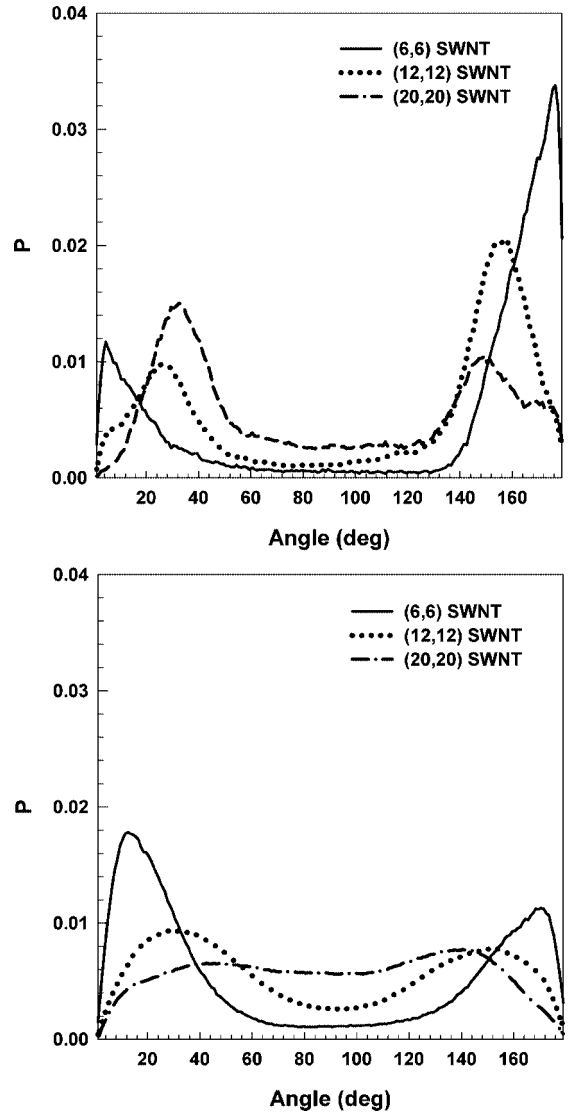

Figure 3. Probability density for SDS surfactants orientation with respect to the SWNTs axis (top panel), and for SDS−SDS relative orientation (bottom panel). Results are obtained for the systems shown in Figure 1, in which the surfactants surface density is ~0.98 nm^2 per headgroup.

SWNTs axis, they form slanted angles on the other two nanotubes, and as the nanotube radius increases the preferred orientation seems to be along one of the three β symmetry axes of graphite. Note that in the SWNTs considered here the nanotube axis is parallel to one of the three α symmetry axes of the graphene sheet rolled up to form the nanotube. Because of the competition between the energetic advantage of maximizing the number of contacts between the SDS tail and the carbon atoms on the SWNTs surface, and the energetic penalty of bending the SDS molecule to wrap the SWNTs, it is likely that the ratio between the SWNTs diameter and the surfactant length is among the dominant parameters that determine how the SDS surfactants orient with respect to the nanotube. In fact, as the SWNTs diameter increases the energetic penalty due

to bending the SDS molecule around the SWNTs decreases. Also, when one SDS molecule lies along one of the β symmetry axes (which forms an angle of 30° with respect to the SWNTs axes) the number of contacts between the methyl groups in the surfactant tail and the SWNT carbon atoms increases as the SWNT diameter increases, proving that it is energetically favorable for the SDS surfactants to wrap the (20,20) nanotubes, but not the narrower ones.

At low surface coverage the simulation snapshots of Figure 1 suggest that the SDS surfactants are aligned not only with respect to the SWNTs axis, but also with respect to each other. In the bottom panel of Figure 3 we quantify this observation in terms of probability density as a function of the SDS−SDS angle at low surfactant density (Figure 1). Angles of 0° and 180° represent SDS surfactants parallel, or antiparallel to each other, respectively. The results indicate that the SDS surfactants on the (6,6) SWNTs are highly ordered with respect to each other, but as the nanotube diameter increases it becomes equally probable to observe SDS surfactants forming any angle with respect to each other. These data suggest that at low surface coverage the SDS surfactants prefer to assume random relative orientations, probably because of entropic reasons. However, on narrow SWNTs it is best for the surfactants to lie parallel/antiparallel with respect to each other to avoid the energetic penalties they would encounter should they bend to wrap the nanotubes.

From the results shown in Figure 1 it is also evident that the surfactant head groups in some cases are in contact with the hydrophobic SWNTs surface, which disagrees with the DFT data presented by Patel and Egorov.[25] However, it is likely that as the SDS surface density increases, the surfactant heads protrude more pronouncedly toward the aqueous phase. This possibility is suggested by the snapshots shown in Figure 2, in which systems are presented where the surfactant density is larger than that considered in Figure 1. One clear difference between our results and the surfactant aggregate morphology commonly postulated is that the SDS surfactants do not uniformly cover the SWNTs. This becomes even more striking when we further increase the surface density on the (6,6) SWNTs. Representative simulation snapshots at increasing SDS surface density are shown in Figure 4.

Rather than distributing homogeneously on the SWNTs, the SDS surfactants form highly disordered admicelles on the nanotubes. These admicelles are not similar in any way to those proposed in 2002 by Poulin *et al.*,[17] or in 2003 by Islam *et al.*,[16] and those considered in the energetic calculations presented by Matarredona *et al.*[18] but are in qualitative agreement with the neutron scattering data of Yurekli *et al.*[19] Our equilibrium simulations suggest that the pronounced curvature of the solid support prevents the formation of the ordered admicelles that form on graphite. It should however

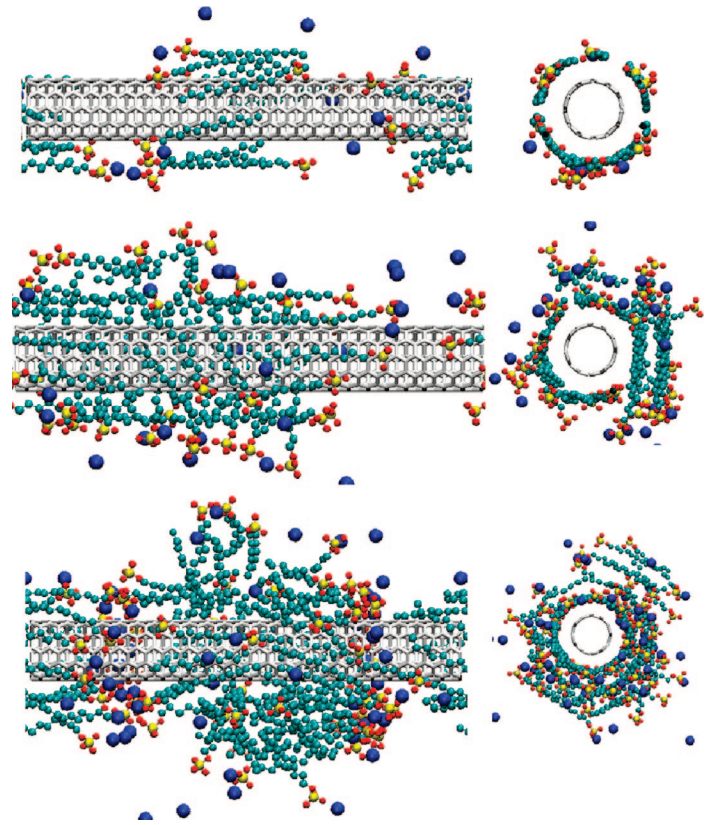

Figure 4. Side (left panels) and front views (right panels) of representative simulation snapshots obtained for SDS surfactants adsorbed on (6,6) SWNTs at increasing surface density. From top to bottom, the surface per surfactant headgroup is 0.98, 0.44, and 0.25 nm^2 respectively. Water molecules are not shown for clarity.

be pointed out that in our simulations the surfactant surface density is chosen arbitrarily. Because the simulations last only for 50 ns, the SDS surfactants may not have had sufficient time to leave the SWNTs, although we observed no evidence for such phenomenon to happen even at the highest surfactant surface densities considered.

Accounting for the actual surfactant aggregate morphology obtained from our realistic simulations should enhance theoretical predictions such as those reported by Patel and Egorov,[25] which are based on a uniform distribution of surfactant tails, surfactant heads, and counterions away from the carbon nanotube surface. However, accounting for nonuniform effects in either self-consistent theories or general theoretical models[32−35] is at present prohibitively expensive. Thus we provide in Figure 5 the density distribution of surfactant head groups (top panels), surfactant tails segments (center panels), and counterions (bottom panels) around the SWNTs. These results correspond to time and space averages of the quantities of interest obtained during our simulations and are a direct consequence of the aggregate morphology discussed above. In the left panels we report the results obtained on the three SWNTs at low SDS surface density (as shown in

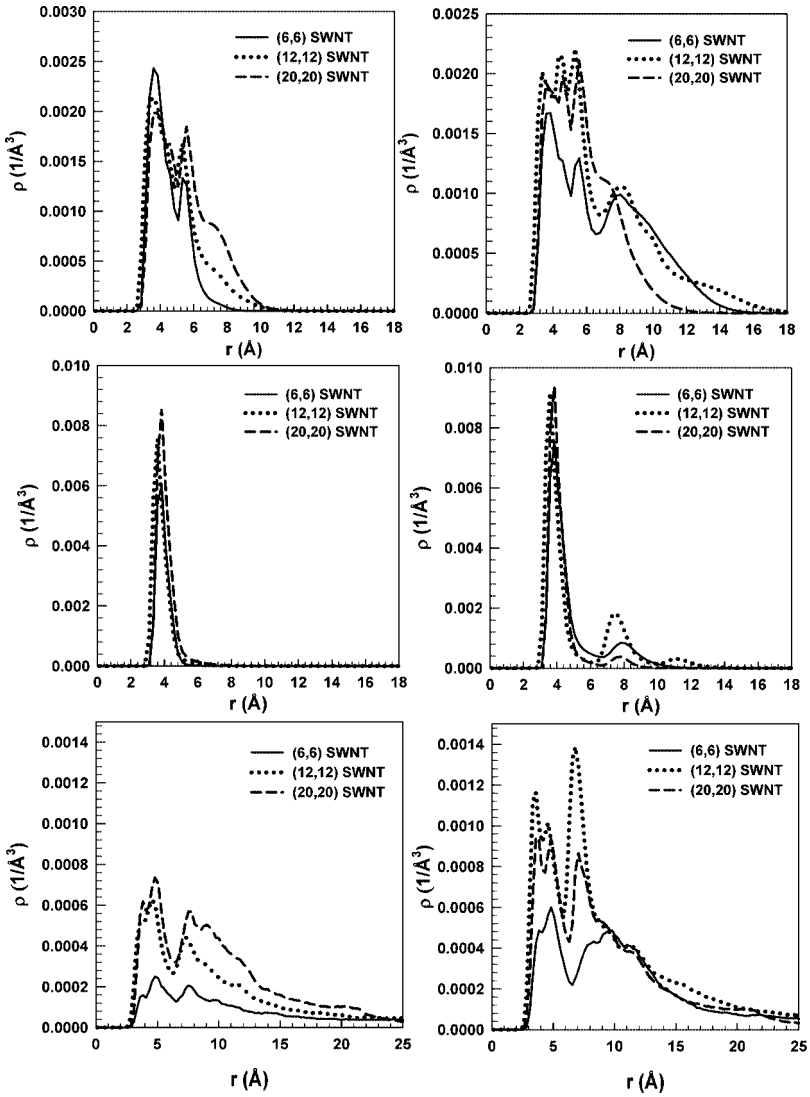

Figure 5. Density profiles of surfactant head groups (top panels), surfactant tail segments (center panels), and counterions (bottom panels) around the SWNTs. In the left panels we report the results obtained on the three SWNTs at low SDS surface density (shown in Figure 1); in the right panels are those obtained at high surface density (shown in Figure 2).

Figure 1); in the right panels are those obtained at high surface density (as shown in Figure 2). In these figures the distance "*r*" is measured radially from the center of the carbon atoms forming the SWNTs. The surfactant head is defined as the center of mass formed by the oxygen atoms and the sulfur atoms in one SDS molecule. One tail segment is either one CH_2 or one CH_3 group in the surfactant tail. From Figure 5, our results suggest that the surfactant tail segments (center panels) accumulate near the hydrophobic SWNTs surfaces, as expected. At low surface density (left panel), we observe the formation of one layer of surfactant tail segments next to the SWNTs, and that the intensity of the peak depends on the nanotube diameter. As the surfactant density increases (right panel) our results suggest the formation of a second shell of surfactant tail segments around the nanotubes, as was indicated by the simulation snapshots of Figure 2. In the case of SDS surfactants on the (12,12) SWNTs our results suggest the formation of up to three layers of surfactant tail segments around the SWNTs. Visual analysis of the simulation snapshots in Figure 2, however, indicates that these layers are not uniform.

The density profiles obtained for the head groups (top panels) do not seem to depend significantly on the SWNT diameter, especially at low surfactant surface density (left panel). Our results indicate that the first peak in the density profile is found at ~0.4 nm from the center of the carbon atoms on the nanotube surface. When excluded-volume effects are considered, this distance corresponds to the head groups being at contact with the hydrophobic SWNTs surfaces, which was not an expected result. As the surfactant surface density increases (right panel) the surfactant heads extend toward the aqueous phase, but our results indicate that a significant probability exists of finding SDS heads at contact with the nanotube surfaces at all conditions considered here, which is in partial agreement with our simulations for aqueous SDS surfactants on graphite.

The results obtained for the counterion density profiles (bottom panels) show a few unexpected features. The SWNTs are not charged, thus they should not attract ionic species. However, because of the SDS adsorption, it is natural for the counterions to be attracted by the surfactant heads. Indeed the first peak in the counterion density profiles is observed at slightly larger separations *r* than those at which the first peak in the headgroup density profile was observed. It is interesting to point out that the intensity of the first peak in the density profiles for counterions is approximately $^1/_2$ of that for the first peak in the density profile for the surfactant heads. This happens because one counterion coordinates simultaneously with multiple surfactant heads, a manifestation of the counterion condensation phenomenon. It is also worth pointing out that the counterion densities show slowly decaying profiles as the distance *r* increases further from the first intense peaks. These results demonstrate that SWNT-SDS complexes can be thought of as polyanions, in which counterion condensation does not manage to neutralize the entire complex charge, as explained by Manning.[33,34,36] It has been recently demonstrated experimentally by Niyogi *et al.*[12] that understanding how the density and the morphology of the adsorbed aggregates vary with the addition of electrolytes to the aqueous systems may lead to enhanced separation strategies.

CONCLUSIONS

In conclusion, we reported the first detailed all-atom simulation studies for the morphology of SDS surfactants adsorbed on (6,6), (12,12), and (20,20) single-walled carbon nanotubes. Our results agree with and augment previous neutron scattering experimental data and show that the morphology of the surfactant aggregates strongly depends on the nanotube diameter, as well as on the surface coverage. The additional molecular-level information provided by our results (*i.e.*, density profiles for surfactant tails, surfactant heads, and counterions away from the nanotube surface) should be accounted for to better understand how adsorbed surfactants affect the effective carbon nanotube−carbon nanotube potential of mean force in aqueous solutions, to improve the stability of aqueous SWNTs dispersions, and to design enhanced separation procedures such as ultracentrifugation. We demonstrated that intrinsic surfactant properties such as the flexibility of each individual surfactant molecule are important, in addition to surfactant−surfactant and surfactant−nanotube interactions to determine the equilibrium morphology of the adsorbed surfactant aggregates. Our results are useful for implementing coarse-grained models that will allow us to calculate the equilibrium adsorption isotherms for SDS surfactants on SWNTs of various diameters.

SIMULATION DETAILS

Aqueous SDS surfactants were simulated at contact with (6,6), (12,12), and (20,20) single-walled carbon nanotubes. Within these substrates, the carbon atoms, treated as Lennard-Jones spheres, were maintained rigid throughout the course of the simulations. Water molecules were modeled using the SPC/E model. The details of the force field employed are described in ref 20. Dispersive attractions and repulsive interactions were treated with an inner cutoff of 0.8 nm and outer cutoff of 1.0 nm. Long-range electrostatic interactions were treated using the particle mesh Ewald (PME) method.[37] Bond lengths and bond angles in water were maintained fixed using the SETTLE algorithm.[38]

The simulation package GROMACS, version 3.3.3,[39−41] was employed to integrate the equations of motion. The number of particles (N), the simulation box volume (V), and the temperature (T) were maintained constant during our simulations. In all simulations the time step was 2 fs. The Nose−Hoover thermostat[42] with leapfrog algorithm[42] was implemented with a relaxation time constant of 100 fs. All simulations were conducted for 50 ns, and only the last 10 ns were used for data analysis. The systems are considered equilibrated because the results do not change during the last 30 ns of simulations. Although the length of the simulation, which approaches the limit of available computation resources, does not allow us to assess the number of surfactant molecules adsorbed at equilibrium as a function of bulk surfactant concentration, the number of surfactants simulated on each SWNT is consistent with available experimental data. In all the simulations considered one SWNT was placed in the center of the simulation box with the axis aligned along the Z direction. In the initial configuration the desired number of surfactants were placed around the SWNT with their tails parallel to the nanotube axis. The number of water molecules in the box was adjusted to reproduce the bulk water density. Periodic boundary conditions were employed in X, Y, and Z dimensions. Further details are given in Table 1.

TABLE 1. Simulation Details for the Systems Studied in This Work

substrate	number of SDS	surfactant coverage (nm^2/headgroup)	box size (nm^3)	number of water molecules
(6,6)	16	0.98	7.0 × 7.0 × 6.1487	9900
(12,12)	32	0.98	7.0 × 7.0 × 6.1487	8640
(20,20)	53	0.98	7.0 × 7.0 × 6.1487	7700
(6,6)	36	0.44	7.0 × 7.0 × 6.1487	9000
(12,12)	64	0.49	7.0 × 7.0 × 6.1487	8450
(20,20)	64	0.81	7.0 × 7.0 × 6.1487	7700
(6,6)	64	0.25	7.0 × 7.0 × 6.1487	8800

Acknowledgment. The authors acknowledge financial support from the US DoE under contract no. FG02-06ER64239, and from the Oklahoma State Regents for Higher Education. Generous allocations of computing time were provided by the OU Supercomputing Center for Education and Research (OSCER) and by the National Energy Research Scientific Computing Center (NERSC) at Lawrence Berkeley National Laboratory. The authors are grateful to M. Riello and D. Catapano for conducting some of the simulations discussed here and to B. Grady for helpful discussions.

REFERENCES AND NOTES

1. Shaffer, M. S. P.; Windle, A. H. Fabrication and Characterization of Carbon Nanotube/Poly(vinyl alcohol) Composites. *Adv. Mater.* **1999**, *11*, 937–941.
2. Vigolo, B.; Poulin, P.; Lucas, M.; Launois, P.; Bernier, P. Improved Structure and Properties of Single-Wall Carbon Nanotube Spun Fibers. *Appl. Phys. Lett.* **2002**, *81*, 1210–1212.
3. Cadek, M.; Coleman, J. N.; Barron, V.; Hedicke, K.; Blau, W. J. Morphological and Mechanical Properties of Carbon-Nanotube-Reinforced Semicrystalline and Amorphous Polymer Composites. *Appl. Phys. Lett.* **2002**, *81*, 5123–5125.
4. Peters, J. E.; Papavassiliou, D. V.; Grady, B. P. Unique Thermal Conductivity Behavior of Single-Walled Carbon Nanotube-Polystyrene Composites. *Macromolecules* **2008**, *41*, 7274–7277.
5. Nikolaev, P.; Bronikowski, M. J.; Bradley, R. K.; Rohmund, F.; Colbert, D. T.; Smith, K. A.; Smalley, R. E. Gas-Phase Catalytic Growth of Single-Walled Carbon Nanotubes from Carbon Monoxide. *Chem. Phys. Lett.* **1999**, *313*, 91–97.
6. Bronikowski, M. J.; Willis, P. A.; Colbert, D. T.; Smith, K. A.; Smalley, R. E. Gas-Phase Production of Carbon Single-Walled Nanotubes From Carbon Monoxide *via* the Hipco Process: A Parametric Study. *The 47th International Symposium: Vacuum, Thin Films, Surfaces/Interfaces, and Processing*; NAN06: Boston, MA, 2001; pp 1800−1805.
7. Kitiyanan, B.; Alvarez, W. E.; Harwell, J. H.; Resasco, D. E. Controlled Production of Single-Wall Carbon Nanotubes by Catalytic Decomposition of CO on Bimetallic Co-Mo Catalysts. *Chem. Phys. Lett.* **2000**, *317*, 497–503.
8. Iijima, S. Helical Microtubules of Graphitic Carbon. *Nature* **1991**, *354*, 56–58.
9. O'Connell, M. J.; Bachilo, S. M.; Huffman, C. B.; Moore, V. C.; Strano, M. S.; Haroz, E. H.; Rialon, K. L.; Boul, P. J.; Noon, W. H.; Kittrell, C.; Ma, J.; Hauge, R. H.; Weisman, R. B.; Smalley, R. E. Band Gap Fluorescence from Individual Single-Walled Carbon Nanotubes. *Science* **2002**, *297*, 593–596.
10. Arnold, M. S.; Green, A. A.; Hulvat, J. F.; Stupp, S. I.; Hersam, M. C. Sorting Carbon Nanotubes by Electronic Structure Using Density Differentiation. *Nat. Nano* **2006**, *1*, 60–65.

11. Nair, N.; Kim, W. J.; Braatz, R. D.; Strano, M. S. Dynamics of Surfactant-Suspended Single-Walled Carbon Nanotubes in a Centrifugal Field. *Langmuir* **2008**, *24*, 1790–1795.
12. Niyogi, S.; Densmore, C. G.; Doorn, S. K. Electrolyte Tuning of Surfactant Interfacial Behavior for Enhanced Density-Based Separations of Single-Walled Carbon Nanotubes. *J. Am. Chem. Soc.* **2009**, *131*, 1144–1153.
13. O'Connell, M. J.; Boul, P.; Ericson, L. M.; Huffman, C.; Wang, Y.; Haroz, E.; Kuper, C.; Tour, J.; Ausman, K. D.; Smalley, R. E. Reversible Water-Solubilization of Single-Walled Carbon Nanotubes by Polymer Wrapping. *Chem. Phys. Lett.* **2001**, *342*, 265–271.
14. Hagen, A.; Hertel, T. Quantitative Analysis of Optical Spectra from Individual Single-Wall Carbon Nanotubes. *Nano Lett.* **2003**, *3*, 383–388.
15. Wallace, E. J.; Sansom, M. S. P. Carbon Nanotube/Detergent Interactions *via* Coarse-Grained Molecular Dynamics. *Nano Lett.* **2007**, *7*, 1923–1928.
16. Islam, M. F.; Rojas, E.; Bergey, D. M.; Johnson, A. T.; Yodh, A. G. High Weight Fraction Surfactant Solubilization of Single-Wall Carbon Nanotubes in Water. *Nano Lett.* **2003**, *3*, 269–273.
17. Poulin, P.; Vigolo, B.; Launois, P. Films and Fibers of Oriented Single Wall Nanotubes. *Carbon* **2002**, *40*, 1741–1749.
18. Matarredona, O.; Rhoads, H.; Li, Z.; Harwell, J. H.; Balzano, L.; Resasco, D. E. Dispersion of Single-Walled Carbon Nanotubes in Aqueous Solutions of the Anionic Surfactant NaDDBS. *J. Phys. Chem. B* **2003**, *107*, 13357–13367.
19. Yurekli, K.; Mitchell, C. A.; Krishnamoorti, R. Small-Angle Neutron Scattering from Surfactant-Assisted Aqueous Dispersions of Carbon Nanotubes. *J. Am. Chem. Soc.* **2004**, *126*, 9902–9903.
20. Tummala, N. R.; Striolo, A. Role of Counterion Condensation in the Self-Assembly of SDS Surfactants at the Water−Graphite Interface. *J. Phys. Chem. B* **2008**, *112*, 1987–2000.
21. Sammalkorpi, M.; Panagiotopoulos, A. Z.; Haataja, M. Structure and Dynamics of Surfactant and Hydrocarbon Aggregates on Graphite: A Molecular Dynamics Simulation Study. *J. Phys. Chem. B* **2008**, *112*, 2915–2921.
22. Dominguez, H. Self-Aggregation of the SDS Surfactant at a Solid−Liquid Interface. *J. Phys. Chem. B* **2007**, *111*, 4054–4059.
23. Wanless, E. J.; Ducker, W. A. Organization of Sodium Dodecyl Sulfate at the Graphite−Solution Interface. *J. Phys. Chem.* **1996**, *100*, 3207–3214.
24. Ortiz-Acevedo, A.; Xie, H.; Zorbas, V.; Sampson, W. M.; Dalton, A. B.; Baughman, R. H.; Draper, R. K.; Musselman, I. H.; Dieckmann, G. R. Diameter-Selective Solubilization of Single-Walled Carbon Nanotubes by Reversible Cyclic Peptides. *J. Am. Chem. Soc.* **2005**, *127*, 9512–9517.
25. Patel, N.; Egorov, S. A. Dispersing Nanotubes with Surfactants: A Microscopic Statistical Mechanical Analysis. *J. Am. Chem. Soc.* **2005**, *127*, 14124–14125.
26. Striolo, A. Colloidal Brushes in Complex Solutions: Existence of a Weak Midrange Attraction due to Excluded-Volume Effects. *Phys. Rev. E* **2006**, *74*, 041401–11.
27. Striolo, A. Controlled Assembly of Spherical Nanoparticles: Nanowires and Spherulites. *Small* **2007**, *3*, 628–635.
28. Striolo, A. On the Solution Self-Assembly of Nanocolloidal Brushes: Insights from Simulations. *Nanotechnology* **2008**, *19*, 445606.
29. Konatham, D.; Striolo, A. Molecular Design of Stable Graphene Nanosheets Dispersions. *Nano Lett.* **2008**, *8*, 4630–4641.
30. Strano, M. S.; Moore, V. C.; Miller, M. K.; Allen, M. J.; Haroz, E. H.; Kittrell, C.; Hauge, R. H.; Smalley, R. E. The Role of Surfactant Adsorption During Ultrasonication in the Dispersion of Single-Walled Carbon Nanotubes. *J. Nanosci. Nanotechnol.* **2003**, *3*, 81–86.
31. Bandyopadhyay, S.; Shelley, J. C.; Tarek, M.; Moore, P. B.; Klein, M. L. Surfactant Aggregation at a Hydrophobic Surface. *J. Phys. Chem. B* **1998**, *102*, 6318–6322.
32. Anderson, C. F.; Record, M. T. Polyelectrolyte Theories and Their Applications to DNA. *Annu. Rev. Phys. Chem.* **1982**, *33*, 191–222.
33. Manning, G. S. Counterion Binding in Polyelectrolyte Theory. *Acc. Chem. Res.* **1979**, *12*, 443–449.
34. Manning, G. S. Counterion Condensation on Charged Spheres, Cylinders, and Planes. *J. Phys. Chem. B* **2007**, *111*, 8554–8559.
35. Le Bret, M.; Zimm, B. H. Distribution of Counterions Around a Cylindrical Polyelectrolyte and Manning's Condensation Theory. *Biopolymers* **1984**, *23*, 287–312.
36. Manning, G. S. Limiting Laws and Counterion Condensation in Polyelectrolyte Solutions I. Colligative Properties. *J. Chem. Phys.* **1969**, *51*, 924–933.
37. Essmann, U.; Perera, L.; Berkowitz, M. L.; Darden, T.; Lee, H.; Pedersen, L. G. A Smooth Particle Mesh Ewald Method. *J. Chem. Phys.* **1995**, *103*, 8577.
38. Miyamoto, S.; Kollman, P. A. Settle: An Analytical Version of the SHAKE and RATTLE Algorithm for Rigid Water Models. *J. Comput. Chem.* **1992**, *13*, 952–962.
39. Lindahl, E.; Hess, B.; Van Der Spoel, D. GROMACS 3.0: A Package for Molecular Simulation and Trajectory Analysis. *J. Mol. Model.* **2001**, *7*, 306–317.
40. Berendsen, H. J. C.; Van Der Spoel, D.; Van Drunen, R. GROMACS: A Message-Passing Parallel Molecular Dynamics Implementation. *Comput. Phys. Commun.* **1995**, *91*, 43–56.
41. Van Der Spoel, D.; Lindahl, E.; Hess, B.; Groenhof, G.; Mark, A. E.; Berendsen, H. J. C. GROMACS: Fast, Flexible, and Free. *J. Comput. Chem.* **2005**, *26*, 1701–1718.
42. Frenkel, D.; Smit, B. *Understanding Molecular Simulations: From Algorithms to Applications*; Academic Press: San Diego, CA, 1996; Vol. 1.